Dynamic response of a hinged-free beam subjected to impact at an arbitrary location along its span with shear effect

Y. Zhang[†]

*School of Mechanical and Electrical Engineering, Beijing University of Chemical Technology,
P.O. Box 93, Beijing, 100029, P. R. China*

J. L. Yang[‡]

*Solid Mechanics Research Center, Beijing University of Aeronautics and Astronautics,
Beijing, 100083, P. R. China*

Abstract. In case of considering the shear effect, the complete solutions are obtained for dynamic plastic response of a rigid, perfectly plastic hinged-free beam, of which one end is hinged and the other end free, subjected to a transverse strike by a travelling rigid mass at an arbitrary location along its span. Special attention is paid to new deformation mechanisms due to shear sliding on both sides of the rigid mass and the plastic energy dissipation. The dimensionless numerical results demonstrate that three parameters, i.e., mass ratio, impact position of mass, as well as the non-dimensional fully plastic shear force, have significant influence on the partitioning of dissipated energy and failure mode of the hinged-free beam. The shear effect can never be negligible when the mass ratio is comparatively small and the impact location of mass is close to the hinged end.

Keywords: hinged-free beam; impact; plastic dissipated energy; deformation mechanism; complete solution.

1. Introduction

The rigid, perfectly plastic material idealization has been widely adopted to study the dynamic behavior of structures subjected to intensive dynamic loading. In this case, according to bending only theory the initial transverse shear forces are infinitely large at the boundaries of loading zones, and exceed the fully plastic shear force of the beam cross-section. It appears that the transverse shear forces may exercise a more important role in the response of dynamically loaded rigid, perfectly plastic structures (Norman Jones 1989, Stronge and Yu 1993). Indeed, structures may fail due to excessive transverse shear sliding.

† Lecturer, Assistant Professor, E-mail: zhangya@mail.buct.edu.cn
‡ Professor, E-mail: jlyang@buaa.edu.cn

Several authors have examined the influence of the transverse shear on the dynamic behavior of rigid, perfectly plastic structures. Using the rigid, perfectly plastic idealization and approximate square yield curve in shear force-bending moment plane, Jones and Song (1986) examined in detail the dynamic plastic response of a rigid, perfectly plastic simply supported beam subjected to the blast pressure loading uniformly distributed over a portion of the span. Various initial mechanisms of deformation, for a wide range of parameters, are obtained. Yu (1993) examined the shear failure of a cantilever beam with an attached mass at the tip. Liu and Jones (1988, 1987) presented the theoretical analyses and experimental results to examine the deformation and failure of rigid, perfectly plastic fully clamped beams struck transversely by a mass at any point on the span with shear effect. Lellep and Torn (2005) discussed the shear and bending response of a rigid-plastic beam clamped at the left and simply supported at the right-hand end. Li and Jones (1999) presented an analytical model to study the shear and adiabatic shear failure in a clamped beam under impulsive pressure loadings. Yu and Chen (2000) re-examined the plastic shear failure at the supports of clamped beams loaded impulsively, and discuss the effect of the interaction between the shear force and bending moment. Li and Jones (1994, 1995) have studied the dynamic plastic response of fully clamped circular plates and cylindrical shells when transverse shear effects are taken into account.

In the investigations cited above the beam structures under considerations often are free-free beam, cantilever beam, simply supported or fully clamped beam, respectively. However, between the cases of simply supported beam and free-free beam, there is another kind of beam which is simply supported or hinged at one end and free at the other end, and is called hinged-free beam as same as in Zhang and Yang (2002). The hinged-free beam can often be seen in engineering structures, for example in the research for pipe systems and rotors of helicopters. A bending only theory of dynamic plastic analysis of hinged-free beams subjected to a transverse strike by a travelling rigid mass at an arbitrary location along its span has been given in Zhang and Yang (2002). By reviewing the previous studies, however, it seems that no attempt has so far been made to study the influence of transverse shear force on the dynamic behavior of the hinged-free beam. In this paper, the shear and bending response of the hinged-free beam subjected to transversely impact by a mass at an arbitrary location along its span is examined, and shear sliding on both sides of the mass and shear failure are investigated particularly.

2. Theoretical analysis

2.1 Theoretical model

Consider a rigid, perfectly plastic hinged-free beam subjected to strike by a mass G travelling with an initial velocity v_0, at an interior cross section, A, l_a from the simply support as shown in Fig. 1. The beam has a length $l_a + l_b = l$ and mass per unit length m. It is assumed that after impact the mass remains attached to the beam during the entire response process. The square yield curve presented in Fig. 2 will be used to control the plastic yielding of the beam.

For convenience in the derivations in the following sections, following dimensionless variables are introduced
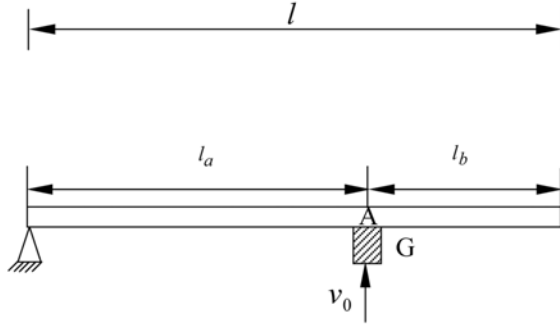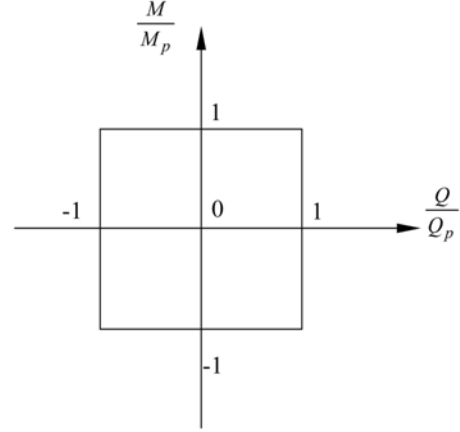
Fig. 1 A hinged-free beam struck by a mass G

Fig. 2 Plastic yield surface

$$\eta_1 = \frac{l_a}{l}, \quad \eta_2 = \frac{l_b}{l}, \quad \tilde{u} = \frac{u}{l}, \quad g = \frac{G}{ml}, \quad \Lambda = \frac{Gv_0^2}{2M_p}, \quad \hat{E}_b = \frac{E_b}{M_p}, \quad \hat{E}_s = \frac{E_s}{M_p}, \quad \hat{E}_k = \frac{E_k}{M_p}$$

$$q = \frac{Ql}{M_p}, \quad \tau = t\sqrt{\frac{M_p}{ml^3}}, \quad (\overset{\circ\circ}{}) = \frac{d^2}{d\tau^2}(\ ), \quad (\overset{\circ}{}) = \frac{d}{d\tau}(\ ), \quad v = Q_p l/2M_p \tag{1'}$$

where M_p and Q_p denote the fully plastic bending moment and the fully plastic shear force of the beam. E_b, E_s and E_k stand for the plastic bending dissipated energy, plastic shear sliding energy and the kinetic energy of rigid-body motion, respectively. Parameter v, the ratio of shear strength to bending strength, is called as non-dimensional fully plastic shear force. When the finite shear strength of a beam is considered, it is known from (Jones 1989) that the transverse velocity profile of a beam may change with the magnitude of v.

2.2 Deformation mechanisms during the initial response of the beam

The initial deformation mechanisms are controlled by parameters that relate to impact position η_1 and non-dimensional parameter v. Six different initial deformation mechanisms as shown in Fig. 3 are found when the shear sliding on both sides of mass G are considered and that on the simply support is neglected for $1/3 < \eta_1 \leq 1$. In Fig. 3, A_b, H_1 and H_2 are bending only hinges, respectively. A_{b-s} is a generalized plastic hinge controlled by bending moment and shear force. A_s denotes plastic hinge in which only transverse shear sliding occurs. The map of initial deformation mechanisms in $v - \eta_1$ plane is shown in Fig. 4.

It is clear from Fig. 4 that, deformation mechanism $H_1 - A_{b-s} - H_2$ is the most general and complicated one among them. It will be seen in the following sections that the evolution of the mechanism $H_1 - A_{b-s} - H_2$ will experience most of the other deformation mechanisms during the response process. Therefore, the derivations of the governing equations are focused on deformation mechanism $H_1 - A_{b-s} - H_2$ only. The governing equations for the other five initial deformation mechanisms are given briefly in Appendix A, and theoretical analysis for the dynamic behavior of a hinged-free beam struck by a rigid mass at free end can be found in Appendix B.
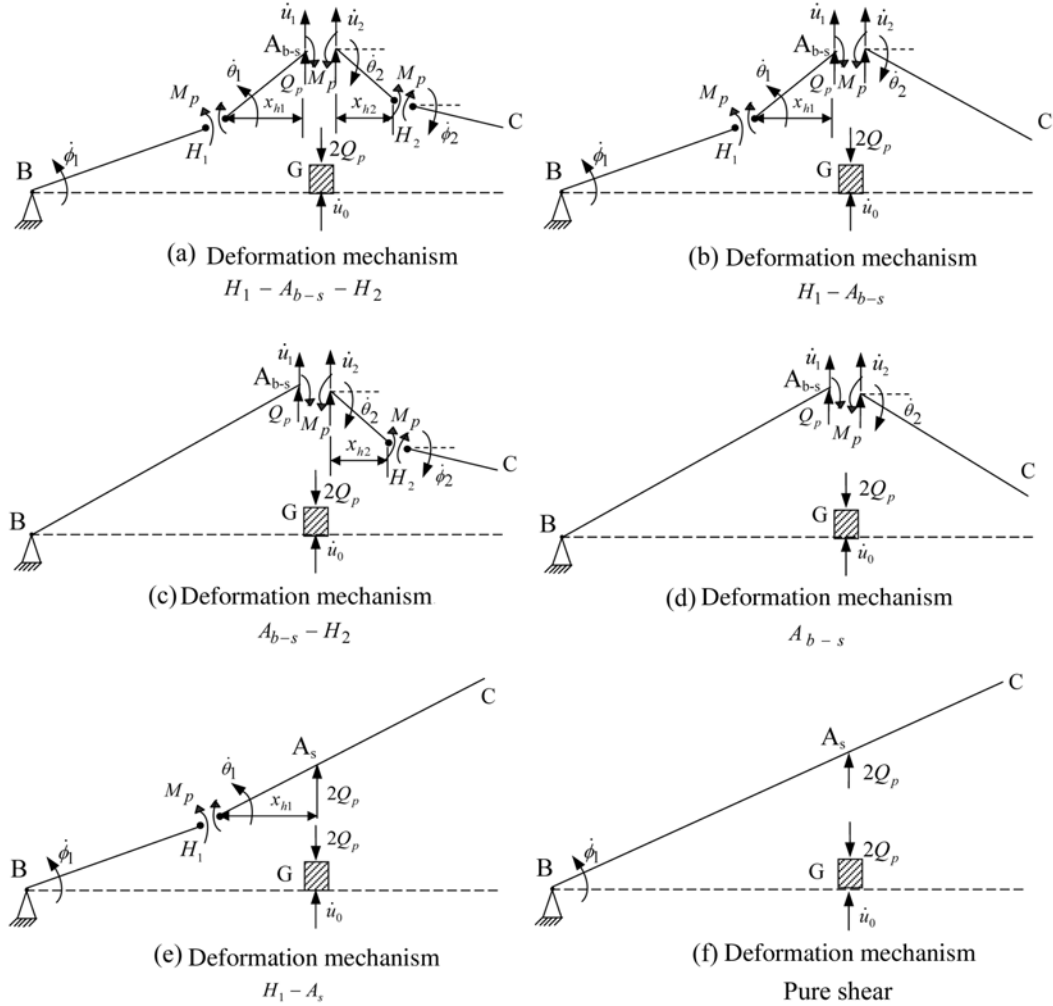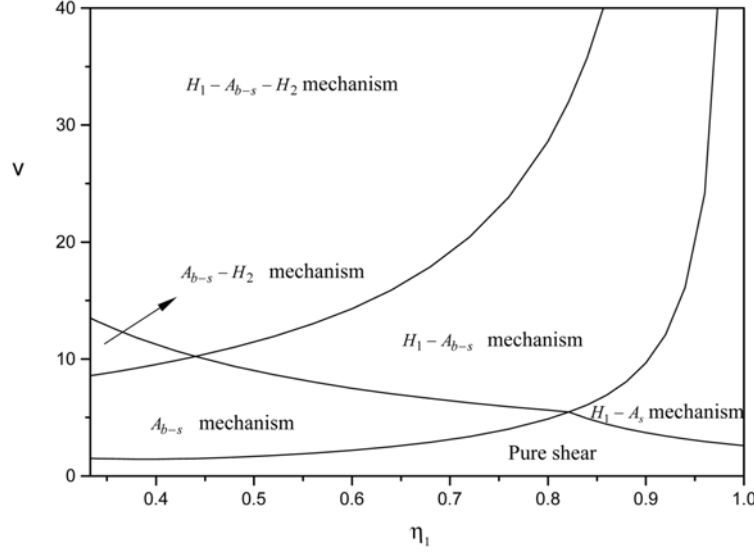
Fig. 3 Possible deformation mechanisms

2.3 Analysis of the entire response for initial deformation mechanism $H_1 - A_{b-s} - H_2$

2.3.1 Phase 1: $0 < \tau \leq \tau_1$

The velocity diagram for initial deformation mechanism $H_1 - A_{b-s} - H_2$ is shown in Fig. 3(a), in which there are a generalized plastic hinge A_{b-s}, and plastic bending hinges H_1 and H_2 at each side of the impact point, respectively. It is known from (Norman Jones 1989, Stronge and Yu 1993) that after impact, transverse shear sliding occurs on both sides of mass G, and the plastic bending hinges H_1 and H_2 are stationary because the shear forces at shear sliding section are assumed to keep invariable until shear sliding ceases. In Fig. 3(a), $\dot{u}_1$ and $\dot{u}_2$ are the upward velocities on the left- and right-hand sides adjacent to the impact point, respectively. $\dot{\theta}_1$, $\dot{\phi}_1$, $\dot{\theta}_2$ and $\dot{\phi}_2$ denote the absolute angular velocities of segments H_1A, BH_1, AH_2 and H_2C, respectively. According to the equilibrium conditions for these segments, the non-dimensional equations of motion for deformation mechanism $H_1 - A_{b-s} - H_2$ can be expressed as

Fig. 4 The map of initial deformation mechanisms in $v-\eta_1$ plane

$$(\eta_1 - \xi_1)^3 \overset{\circ\circ}{\phi}_1 = 3 \tag{1.1}$$

$$\xi_1(2\overset{\circ\circ}{\tilde{u}}_1 - \xi_1\overset{\circ\circ}{\theta}_1) = 4v \tag{1.2}$$

$$\xi_1^2(3\overset{\circ\circ}{\tilde{u}}_1 - 2\xi_1\overset{\circ\circ}{\theta}_1) = 12 \tag{1.3}$$

$$\overset{\circ\circ}{\tilde{u}}_1 - \xi_1\overset{\circ\circ}{\theta}_1 - (\eta_1 - \xi_1)\overset{\circ\circ}{\phi}_1 = 0 \tag{1.4}$$

$$(\eta_2 - \xi_2)^3 \overset{\circ\circ}{\phi}_2 = 12 \tag{1.5}$$

$$\xi_2(2\overset{\circ\circ}{\tilde{u}}_2 - \xi_2\overset{\circ\circ}{\theta}_2) = 4v \tag{1.6}$$

$$\xi_2^2(3\overset{\circ\circ}{\tilde{u}}_2 - 2\xi_2\overset{\circ\circ}{\theta}_2) = 12 \tag{1.7}$$

$$\overset{\circ\circ}{\tilde{u}}_2 - \xi_2\overset{\circ\circ}{\theta}_2 - \frac{1}{2}(\eta_2 - \xi_2)\overset{\circ\circ}{\phi}_2 = 0 \tag{1.8}$$

The equations can be recast as

$$\overset{\circ\circ}{\tilde{u}}_1 = \frac{4(2v\xi_1 - 3)}{\xi_1^2}, \quad \overset{\circ\circ}{\theta}_1 = \frac{12(v\xi_1 - 2)}{\xi_1^3}, \quad \overset{\circ\circ}{\phi}_1 = \frac{3}{(\eta_1 - \xi_1)^3} \tag{2}$$

$$\overset{\circ\circ}{\tilde{u}}_2 = \frac{4(2v\xi_2 - 3)}{\xi_2^2}, \quad \overset{\circ\circ}{\theta}_2 = \frac{12(v\xi_2 - 2)}{\xi_2^3}, \quad \overset{\circ\circ}{\phi}_2 = \frac{12}{(\eta_2 - \xi_2)^3} \tag{3}$$

where $\overset{\circ\circ}{\tilde{u}}_1 = \ddot{u}_1 ml^2/M_p, \overset{\circ\circ}{\tilde{u}}_2 = \ddot{u}_2 ml^2/M_p, \xi_1 = x_{h1}/l$ and $\xi_2 = x_{h2}/l$. Besides, ξ_1 and ξ_2 should satisfy

$$4(3 - v\xi_1)(\eta_1 - \xi_1)^2 - 3\xi_1^2 = 0 \tag{4}$$

$$2(3 - v\xi_2)(\eta_2 - \xi_2)^2 - 3\xi_2^2 = 0 \tag{5}$$

The transverse dimensionless acceleration of mass G is

$$\overset{\circ\circ}{\tilde{u}}_0 = -4v/g \tag{6}$$

The initial conditions are as follows

$$\tau = 0, \quad \tilde{u}_0 = \tilde{u}_1 = \tilde{u}_2 = 0, \quad \overset{\circ}{\tilde{u}}_1 = \overset{\circ}{\tilde{u}}_2 = 0, \quad \overset{\circ}{\tilde{u}}_0 = \sqrt{2\Lambda/g}$$

$$\theta_1 = \theta_2 = \overset{\circ}{\theta}_1 = \overset{\circ}{\theta}_2 = 0, \quad \phi_1 = \overset{\circ}{\phi}_1 = \phi_2 = \overset{\circ}{\phi}_2 = 0 \tag{7}$$

Linear ordinary differential Eqs. (2), (3), (6) with initial conditions (7) and relations (4, 5) can be solved numerically.

Phase 1 terminates when the shear sliding on the right-hand side or the left-hand of the impact point ceases. Which case takes place actually depends on the magnitudes of parameters v and η_1.

(a) When $\overset{\circ}{\tilde{u}}_1 = \overset{\circ}{\tilde{u}}_0$ at $\tau_1 = \xi_1^2\sqrt{2\Lambda g}/4g(2v\xi_1 - 3) + 4v\xi_1^2$, the shear sliding on the left-hand side of the impact point stops firstly, while shear sliding on the right-hand side of mass G continues. At the end of Phase 1, the variables of the left-hand side of the beam are as follows

$$\tilde{u}_1 = \frac{2(2v\xi_1 - 3)}{\xi_1^2}\tau_1^2, \quad \overset{\circ}{\tilde{u}}_1 = \frac{4(2v\xi_1 - 3)}{\xi_1^2}\tau_1, \quad \theta_1 = \frac{6(v\xi_1 - 2)}{\xi_1^3}\tau_1^2$$

$$\overset{\circ}{\theta}_1 = \frac{12(v\xi_1 - 2)}{\xi_1^3}\tau_1, \quad \overset{\circ}{\phi}_1 = \frac{3}{(\eta_1 - \xi_1)^3}\tau_1, \quad \phi_1 = \frac{3}{2(\eta_1 - \xi_1)^3}\tau_1^2 \tag{8}$$

The variables of the right-hand side of the beam are as follows

$$\overset{\circ}{\tilde{u}}_2 = \frac{4(2v\xi_2 - 3)}{\xi_2^2}\tau_1, \quad \tilde{u}_2 = \frac{2(2v\xi_2 - 3)}{\xi_2^2}\tau_1^2, \quad \theta_2 = \frac{12(v\xi_2 - 2)}{\xi_2^3}\tau_1$$

$$\theta_2 = \frac{6(2v\xi_2 - 2)}{\xi_2^3}\tau_1^2, \quad \overset{\circ}{\phi}_2 = \frac{12}{(\eta_2 - \xi_2)^3}\tau_1, \quad \phi_2 = \frac{6}{(\eta_2 - \xi_2)^3}\tau_1^2 \tag{9}$$
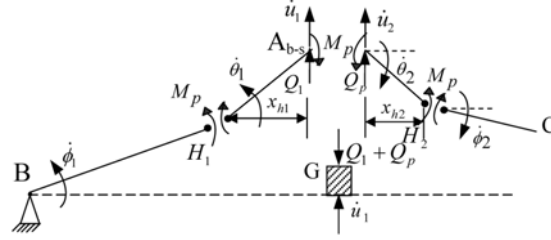
The displacement and velocity of mass G are as follows

$$\tilde{u}_0 = \frac{\sqrt{2\Lambda g}\,\tau_1 - 2v\tau_1^2}{g}, \quad \overset{\circ}{\tilde{u}}_0 = \frac{\sqrt{2\Lambda g} - 4v\tau_1}{g} \tag{10}$$

The final sliding displacement at the left-hand side of mass G is

$$S_l = \tilde{u}_0(\tau_1) - \tilde{u}_1(\tau_1) \tag{11}$$

(b) When $\overset{\circ}{\tilde{u}}_2 = \overset{\circ}{\tilde{u}}_0$ at $\tau_1 = \xi_2^2\sqrt{2\Lambda g}/4g(2v\xi_2 - 3) + 4v\xi_2^2$, the shear sliding on the right-hand side of the impact point stops firstly, while shear sliding on the left-hand side of the impact point continues. At the end of Phase 1, the variables of the beam and rigid mass are the same as Eqs. (8)-

Fig. 5 Possible velocity diagram in phase 2 for $H_1 - A_{b-s} - H_2$

(10) but with $\tau_1 = \xi_2^2 \sqrt{2\Lambda g}/4g(2v\xi_2 - 3) + 4v\xi_2^2$. The final sliding displacement at the right-hand side of the impact point is

$$S_R = \tilde{u}_0(\tau_1) - \tilde{u}_2(\tau_1) \tag{12}$$

2.3.2 Phase 2 $\tau_1 < \tau \leq \tau_2$

Case (1): If the shear sliding on the left-hand side of mass G ceases firstly at the end of Phase 1, then the subsequent deformation mechanism is shown in Fig. 5, in which hinge H_1 is a travelling plastic hinge and ξ_1 is a function of dimensionless time τ. The governing equations of segments H_1A and BH_1 are found to be

$$\ddot{\tilde{u}}_1 = \ddot{\tilde{u}}_0 = -\frac{4(2v\xi_1 + 3)}{\xi_1(\xi_1 + 4g)}, \quad \ddot{\theta}_1 = -\frac{12(2g + 2\xi_1 + v\xi_1^2)}{\xi_1^3(\xi_1 + 4g)} \tag{13}$$

$$\ddot{\phi}_1 = \frac{3}{(\eta_1 - \xi_1)^3}, \quad \dot{\xi}_1(\dot{\theta}_1 - \dot{\phi}_1) = \frac{4(6g + 3\xi_1 + v\xi_1^2)}{\xi_1^2(\xi_1 + 4g)} - \frac{3}{(\eta_1 - \xi_1)^2} \tag{14}$$

Eqs. (3) and (5) are still valid for the two segments AH_2 and H_2C in this case. Non-linear ordinary differential Eqs. (3), (13), (14) with initial conditions (8-10) and relation (5) can be solved numerically.

This deformation mechanism is valid until either $\dot{\tilde{u}}_2 = \dot{\tilde{u}}_1 = \dot{\tilde{u}}_0$ or $\dot{\theta}_1 - \dot{\phi}_1 = 0$ at $\tau = \tau_2$, i.e., when the transverse shear sliding on the right-hand side of mass G stops or plastic hinge H_1 vanishes.

(a) When $\dot{\tilde{u}}_2 = \dot{\tilde{u}}_1 = \dot{\tilde{u}}_0$ at $\tau = \tau_2$, the shear sliding on the right-hand side of the impact point ceases. The plastic hinge H_2 will be a travelling hinge during the subsequent motion. Analysis for the subsequent motion is the same as that given in section 2.1 in Zhang and Yang (2002) and not repeated in this paper. The final sliding displacement at the right-hand side of the impact point is
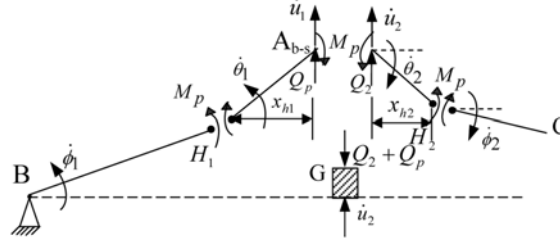
$$S_R = \tilde{u}_0(\tau_2) - \tilde{u}_2(\tau_2) \tag{15}$$

The non-dimensional plastic shear sliding energy is

$$\hat{E}_s = 2v(S_l + S_R) \tag{16}$$

where S_l and S_R are defined by Eqs. (11) and (15), respectively.

The dimensionless plastic bending dissipated energy can be calculated from

Fig. 6 Possible velocity diagram in phase 2 for $H_1 - A_{b-s} - H_2$

$$\hat{E}_b = \Lambda - \hat{E}_s - \frac{3g\eta_1^2}{1 + 3g\eta_1^2} \tag{17}$$

(b) When $\overset{\circ}{\theta}_1 - \overset{\circ}{\phi}_1 = 0$ at $\tau = \tau_2$, the plastic hinge H_1 vanishes, while the shear sliding on the right-hand side of the impact point continues.

Case (2): If the shear sliding on the right-hand side of the impact point ceases first at the end of Phase1, then the subsequent deformation mechanism is shown in Fig. 6, in which hinge H_2 is a travelling plastic hinge and ξ_2 varies with time τ. The governing equations of segments H_2A and H_2C are

$$\overset{\circ\circ}{\tilde{u}}_2 = \overset{\circ\circ}{\tilde{u}}_0 = -\frac{4(2v\xi_2 + 3)}{\xi_2(\xi_2 + 4g)}, \quad \overset{\circ\circ}{\theta}_2 = -\frac{12(2g + 2\xi_2 + v\xi_2^2)}{\xi_2^3(\xi_2 + 4g)} \tag{18}$$

$$\overset{\circ\circ}{\phi}_2 = \frac{12}{(\eta_2 - \xi_2)^3}, \quad \overset{\circ}{\xi}_2(\overset{\circ}{\theta}_2 - \overset{\circ}{\phi}_2) = \frac{4(6g + 3\xi_2 + v\xi_2^2)}{\xi_2^2(\xi_2 + 4g)} - \frac{6}{(\eta_2 - \xi_2)^2} \tag{19}$$

Eqs. (2) and (4) are still valid for the two segments AH_1 and H_1B in this case. With initial conditions obtained from the instant state when Phase 1 terminates and relation (4), non-linear ordinary differential Eqs. (2), (18), (19) can be solved numerically.

This Phase ends when either $\overset{\circ}{\tilde{u}}_2 = \overset{\circ}{\tilde{u}}_1 = \overset{\circ}{\tilde{u}}_0$ or $\overset{\circ}{\theta}_2 - \overset{\circ}{\phi}_2 = 0$ at $\tau = \tau_2$, i.e., when the transverse shear sliding on the left-hand side of the impact point stops or when the plastic hinge H_1 vanishes.

(a) When $\overset{\circ}{\tilde{u}}_2 = \overset{\circ}{\tilde{u}}_1 = \overset{\circ}{\tilde{u}}_0$ at $\tau = \tau_2$, the plastic hinge H_1 will be a travelling hinge during the subsequent motion. Analysis for the subsequent motion is the same as that described in section 2.1 in Zhang and Yang (2002). The final sliding displacement at the left-hand side of the impact point is

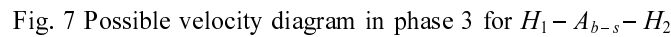$$S_l = \tilde{u}_0(\tau_2) - \tilde{u}_1(\tau_2) \tag{20}$$

The non-dimensional plastic dissipated shear sliding energy is found to be

$$\hat{E}_s = 2v(S_l + S_R) \tag{21}$$

where S_l and S_R are given by Eqs. (20) and (12), respectively.

The dimensionless plastic dissipated bending energy can be still calculated from Eq. (17) but with $\hat{E}_s$ defined by Eq. (21).

(b) When $\overset{\circ}{\theta}_2 - \overset{\circ}{\phi}_2 = 0$ at $\tau = \tau_2$, the plastic hinge H_2 vanishes, while the shear sliding on the left-hand side of the impact point continues.

Fig. 7 Possible velocity diagram in phase 3 for $H_1 - A_{b-s} - H_2$

2.3.3 Phase 3 $\tau_2 < \tau \le \tau_3$

(1) If phase 2 terminates when $\overset{\circ}{\theta}_1 - \overset{\circ}{\phi}_1 = 0$ at $\tau = \tau_2$ for Case (1), the subsequent deformation mechanism is shown in Fig. 7. Eq. (3) and relation (5) are still valid at the moment. The governing equations of segment BA can be expressed as

$$\overset{\circ\circ}{\tilde{u}}_1 = \overset{\circ\circ}{\tilde{u}}_0 = -\frac{3(2v\eta_1 + 1)}{\eta_1(\eta_1 + 3g)} \tag{22}$$

The initial conditions for Phase 3 are derived from the instant state when Phase 2 terminates. This phase ends when $\overset{\circ}{\tilde{u}}_2 = \overset{\circ}{\tilde{u}}_1 = \overset{\circ}{\tilde{u}}_0$ at $\tau = \tau_3$, i.e., when the transverse shear sliding on the right-hand side of the impact point stops. Plastic hinge H_2 will be a travelling hinge during the subsequent motion. Analysis for the subsequent motion is same as section 2.2 (1) in (Zhang and Yang 2002) and not repeated in this paper. The final sliding displacement at the right-hand side of mass G is

$$S_R = \tilde{u}_0(\tau_3) - \tilde{u}_2(\tau_3) \tag{23}$$

The non-dimensional plastic dissipated shear sliding energy is

$$\hat{E}_s = 2v(S_l + S_R) \tag{24}$$

where S_l and S_R are given by Eqs. (11) and (23).

The dimensionless plastic bending dissipated energy can be still calculated from Eq. (17) but with $\hat{E}_s$ defined by Eq. (24).

(2) If phase 2 terminates as a result of $\overset{\circ}{\theta}_2 - \overset{\circ}{\phi}_2 = 0$ at $\tau = \tau_2$ for Case (2), the subsequent deformation mechanism is shown in Fig. 8. Eqs. (2) and (4) are still valid in this case, and the governing equations of segment CA are given by

Fig. 8 Possible velocity diagram in phase 3 for $H_1 - A_{b-s} - H_2$

$$\overset{\circ\circ}{\tilde{u}}_2 = \overset{\circ\circ}{\tilde{u}}_0 = -\frac{2(4v\eta_2 + 3)}{\eta_2(\eta_2 + 4g)} \tag{25}$$

$$\overset{\circ\circ}{\theta}_2 = -\frac{12(g + \eta_2 + v\eta_2^2)}{\eta_2^3(\eta_2 + 4g)} \tag{26}$$

The initial conditions for this case are derived from the instant state when Phase 2 terminates. This phase ends when $\overset{\circ}{\tilde{u}}_2 = \overset{\circ}{\tilde{u}}_1 = \overset{\circ}{\tilde{u}}_0$ at $\tau = \tau_3$, i.e., when the transverse shear sliding on the left-hand side of the impact point stops. The plastic hinge H_1 will be a travelling hinge during the subsequent motion. Analysis for the subsequent motion is same as section 2.2 (2) in (Zhang and Yang 2002) and not repeated in this paper. The final sliding deformation at the left-hand side of the impact point is

$$S_l = \tilde{u}_0(\tau_3) - \tilde{u}_1(\tau_3) \tag{27}$$

The non-dimensional plastic dissipated shear sliding energy is given by

$$\hat{E}_s = 2v(S_l + S_R) \tag{28}$$

where S_l and S_R are given by Eqs. (27) and (12).

The dimensionless plastic bending dissipated energy can be still calculated from Eq. (17) but with $\hat{E}_s$ defined by Eq. (28).

2.4 Shear failure at impact point

In case of considering the shear effect, there are transverse shear sliding S_l and S_R on the both sides of the impact point. If the shear sliding exceeds some critical value, which can be approximately estimated as the ratio of the thickness of the beam to the length, shear failure is most likely to happen.

3. Numerical calculation and discussion

Special attention is paid to the effect of shear on the final deflection at impact point and energy dissipation and its partitioning. The numerical results for different combinations of mass ratio, impact position and parameter v are shown in Figs. 9-11 graphically. For $\eta_1 = 0.5$ and $\Lambda = 3$, the final deflections at impact point are shown in Fig. 9. In order to make comparison with bending only theory, the results of Zhang and Yang (2002) are also shown in the figure. It indicates in Fig. 9 that the plastic shear sliding hardly has an influence on the final deflection at impact point for $g \geq 2.5$, and the influence becomes increasingly important for $g < 2.5$, especially for small mass ratio. If the plastic shear sliding is not considered, the error of the final deflection at impact point is 94.1% for $v = 5$ and $g = 0.05$, 19.8% for $v = 15$ and $g = 0.05$, and 1.6% for $v = 60$ and $g = 0.05$.
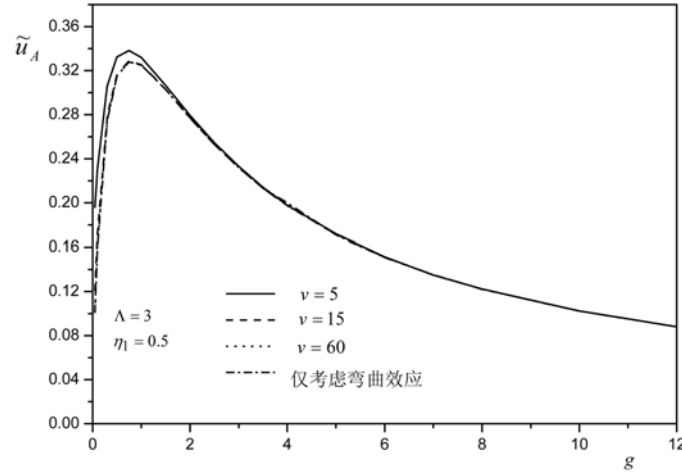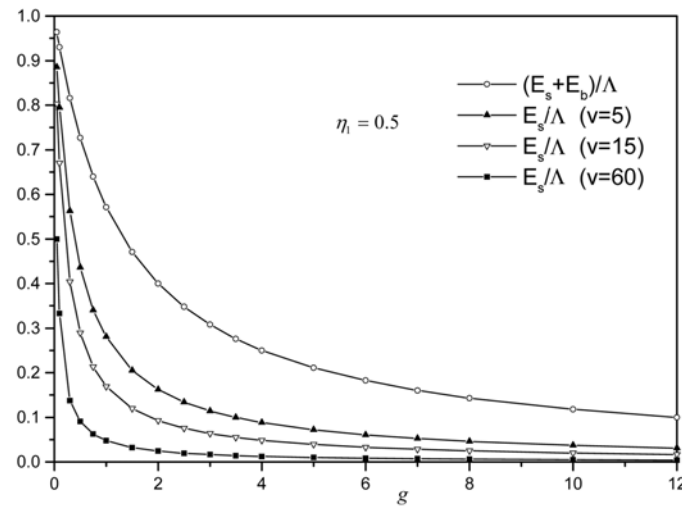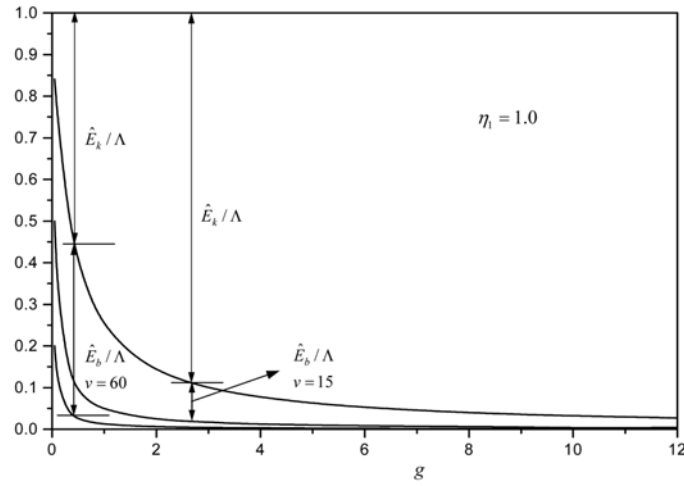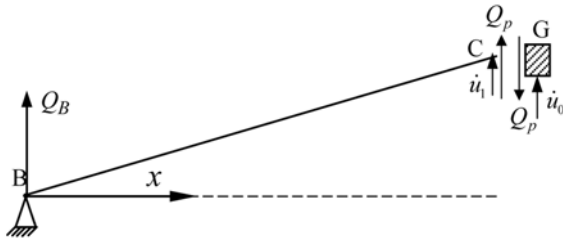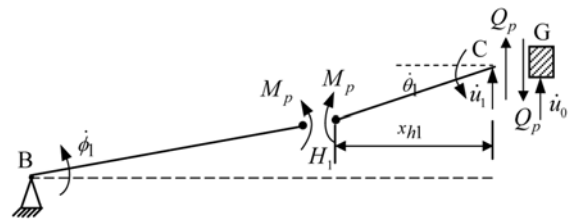
Fig. 9 The final deflection at impact point under given parameters

Fig. 10 Curves of energy partitioning versus mass ratio g

Figs. 10-11 show that the effect of shear on the energy dissipation. It is known that the values of parameter v have no influence on the kinetic energy of rigid-body motion, and have some influence on the partitioning of plastic energy dissipation. The plastic dissipated shear sliding energy increases with the decrease of the mass ratio, so that the shear failure at impact point is more likely to happen for small mass ratio. For $g = 0.3$ and $\eta_1 = 1.0$, i.e., the beam is subjected to impact at the free end, 14.33% of the input energy is dissipated by shear sliding when $v = 15$, but only 4% when $v = 60$. Furthermore, when the impact point is closer to the support, the more of input energy is consumed by shear sliding.

If shear effect on the plastic deformation at simply support of the beam is considered, more initial deformation mechanisms will appear, and can be analyzed in the same way as described above and will not be discussed in this paper.

Fig. 11 Curves of energy partitioning versus g

Fig. 12 Pure shear ($\eta_1 = 1$)   Fig. 13 Initial deformation mechanism H_1 ($\eta_1 = 1$)

4. Conclusions

By using a series of dynamically admissible deformation mechanisms of the structure, the dynamic behavior of a hinged-free beam, of which one end is simply supported or hinged and the other end free, subjected to a transverse strike by a travelling mass at an arbitrary location along its span, is studied in case of considering the shear effect. When $\eta_1 \leq 1/3$, various mechanisms of deformation for combination of shear sliding and plastic bending are obtained for a wide range of parameters. Attention is focused on the influence of the shear effect on the deformation mechanism, final deflection at impact point and energy dissipation. It is concluded that the dynamic behavior of a hinged-free beam with shear effect under consideration, is much more complicated than that of the beam bending only. The present theoretical results expressed in terms of non-dimensional parameters demonstrate that the mass ratio, impact position and parameter v have significant influence on the final deflection at impact point and the partitioning of plastic energy dissipation. When the mass ratio is comparatively large, the effect of shear on the final deflection and partitioning of plastic energy dissipation could be neglected, but not when the mass ratio is comparatively small, nor the impact position of mass is closer to the hinged end of the hinged-free beam.

Acknowledgements

References

Jones, Norman (1989), *Structural Impact*, Cambridge UK: Cambridge University Press.
Jones, Norman and Song, Boquan (1986), "Shear and bending response of rigid-plastic beam to partly distributed blast-type loading", *J. Struct. Mech.*, **14**(3), 275-320.
Lellep, J. and Torn, K. (2005), "Shear and bending response of a rigid-plastic beam subjected to impulsive loading", *Int. J. Impact Eng.*, **31**(9), 1081-1105.
Li, Q.M. and Jones, N. (1994), "Blast loading of fully clamped circular plates with transverse shear effects", *Int. J. Solids Struct.*, **31**(14), 1861-1876.
Li, Q.M. and Jones, N. (1995), "Blast loading of a "short" cylindrical shell with transverse shear effects", *Int. J. Impact Eng.*, **16**(2), 331-353.
Li, Q.M. and Jones, N. (1999), "Shear and adiabatic shear failures in an impulsively loaded fully clamped beam", *Int. J. Impact Eng.*, **22**(6), 589-607.
Liu, J.H. and Jones, N. (1987), "Experimental investigation of clamped beam struck transversely by a mass", *Int. J. Impact Eng.*, **6**(4), 303-335.
Liu, J.H. and Jones, N. (1988), "Dynamic response of a rigid plastic clamped beam struck by a mass at any point on the span", *Int. J. Solids Struct.*, **24**(3), 251-270.
Stronge, W.J. and Yu, T.X. (1993), *Dynamic Models for Structural Plasticity*, Springer-Verlag.
Tongxi, Yu (1993), "Shear failure of a cantilever with an attached mass block at the tip under impulsive loading", *Explosion Shock Waves (in Chinese)*, **13**(2), 97-104.
Yu, T.X. and Chen, F.L. (2000), "A further study of plastic shear failure of impulsively loaded clamped beams", *Int. J. Impact Eng.*, **24**(6-7), 613-629.
Zhang, Y. and Yang, J.L. (2002), "Dynamic plastic response of a hinged-free beam subjected to impact at an arbitrary location along its span", *Struct. Eng. Mech.*, **14**(5), 611-624.

Appendix A

The first phases of dynamic responses for the initial deformation mechanisms other than mechanism $H_1-A_{b-s}-H_2$ are briefly described in this appendix because the evolution of response process is similar to that of mechanism $H_1-A_{b-s}-H_2$. The equation of motion and solutions of travelling mass in Phase 1 are the same as Eqs. (6) and (10) with initial condition given by Eq. (7).

A.1 Initial deformation mechanism: Pure shear
As shown in Fig. 3(f), the dimensionless equation of motion of the beam for pure shear mechanism is

$$\overset{\infty}{\phi}_1 = 12\,v\eta_1 \tag{A.1}$$

The initial condition is $\phi_1 = \overset{\circ}{\phi}_1 = 0$ at $\tau = 0$. The non-dimensional shear force at the simply support is

$$q_B = \frac{Q_B l}{M_p} = 2v(2-3\,\eta_1) \tag{A.2}$$

where Q_B is the shear force at the simply support. When the shear sliding on the simply support does not

occur, it requires $|q_B| < 2v$. This leads to

$$1/3 < \eta_1 \leq 1 \qquad (A.3)$$

As the yield criterion at any point in the beam should not be violated, it follows that the deformation mechanism is valid only when

$$\begin{cases} v \leq v_{c1} = \dfrac{1}{4\eta_1 - 6\eta_1^2 + 2\eta_1^4} & 1/3 < \eta_1 \leq 0.789862 \\[4mm] v \leq v_{c1} = \dfrac{3\sqrt{3}\,\eta_1}{4(3\eta_1 - 2)^{3/2}} & 0.789862 < \eta_1 < 1 \end{cases} \qquad (A.4)$$

A.2 Initial deformation mechanism: $H_1 - A_s$

When $v > v_{c1}$ and $0.789862 < \eta_1 < 1$, a bending plastic hinge may be formed on certain cross section between the simply support and impact point as shown in Fig. 3(e), the dimensionless equations of motion of the beam can be expressed as

$$\overset{\circ\circ}{\phi}_1 = \frac{3}{(\eta_1 - \xi_1)^3} \qquad (A.5)$$

$$\overset{\circ\circ}{\theta}_1 = \frac{3(\xi_1^2 + 4\eta_1\xi_1 - 2\eta_1^2 - 3\eta_2^2)}{(2\eta_2 - \xi_1)(\eta_1 - \xi_1)^2(\eta_2 + \xi_1)^2} \qquad (A.6)$$

where ξ_1 is given by

$$\frac{3}{4(2\eta_2 - \xi_1)}\left[\frac{(\eta_2 + \xi_1)^2}{2(\eta_1 - \xi_1)^2} - 1\right] - v = 0 \qquad (A.7)$$

To satisfy the yield condition, parameter v should satisfy inequality $v_{c1} < v \leq v_{c2}$, where v_{c2} is given by

$$v_{c2} = \frac{3}{4(2\eta_2 - \xi_{1c})}\left[\frac{(\eta_2 + \xi_{1c})^2}{2(\eta_1 - \xi_{1c})^2} - 1\right] \qquad (A.8)$$

Where ξ_{1c} satisfies

$$2 + \frac{\xi_{1c}^2(3\eta_2^3 + 3\eta_2^2\xi_{1c} - \xi_{1c}(\eta_1 - \xi_{1c})^2)}{(\xi_{1c} - 2\eta_2)(\eta_1 - \xi_{1c})^2(\eta_2 + \xi_{1c})^2} = 0 \qquad (A.9)$$

A.3 Initial deformation mechanism: A_{b-s}

When $v > v_{c1}$ and $1/3 < \eta_1 \leq 0.789862$, the bending moment at the impact point will reach the fully plastic bending moment and the deformation mechanism of pure shear may develop into deformation mechanism A_{b-s} as shown in Fig. 3(d). The dimensionless equations of motion of segment BA can be expressed as

$$\overset{\circ\circ}{\tilde{u}}_1 = \frac{3(2v\eta_1 - 1)}{\eta_1^2} \qquad (A.10)$$

The dimensionless equations of motion of segment AC are

$$\overset{\circ\circ}{\tilde{u}}_2 = \frac{2(4v\eta_2 - 3)}{\eta_2^2} \qquad (A.11)$$

$$\overset{\circ\circ}{\theta}_2 = \frac{12(v\eta_2 - 1)}{\eta_2^3} \qquad (A.12)$$

As the yield criterion at any point in the beam should not be violated, the deformation mechanism is valid only when

$$\begin{cases} v_{c1} < v \leq v_{c2} = \dfrac{5.72177}{\eta_2} & 1/3 < \eta_1 \leq 0.440237 \\[2ex] v_{c1} < v \leq v_{c2} = \dfrac{9}{2\,\eta_1} & 0.440237 < \eta_1 \leq 0.789862 \end{cases}$$ (A.13)

A.4 Initial deformation mechanism: $A_{b-s} - H_2$

When $v > v_{c2} = 5.72177/\eta_2$ and $1/3 < \eta_1 \leq 0.440237$, a bending plastic hinge may be formed on certain cross section between impact point and free end for deformation mechanism A_{b-s} as shown in Fig. 3(c). The dimensionless equations of motion of segment BA is the same as Eq. (A.10). The Eqs. (3) and (5) are still valid for the two segments AH_2 and H_2C.

As the yield criterion at any point in the beam should not be violated, the deformation mechanism is valid only when

$$v_{c2} < v \leq v_{c3} = \frac{9}{2\,\eta_1} \qquad 1/3 < \eta_1 \leq 0.440237$$ (A.14)

When $v_{c3} < v$ and $1/3 < \eta_1 \leq 0.440237$, mechanism $H_1 - A_{b-s} - H_2$, which has been discussed in section 2.3 in this paper, is found as shown in Fig. 3(a).

A.5 Initial deformation mechanism: $H_1 - A_{b-s}$

When $v > v_{c2}$ and $0.440237 < \eta_1 \leq 0.789862$, a bending plastic hinge may be formed on certain cross section between the simply support and impact point for initial deformation mechanism A_{b-s}, and a new initial deformation mechanism is found, i.e., $H_1 - A_{b-s}$ as shown in Fig. 3(b). Furthermore, when $v > v_{c2}$ for $0.789862 < \eta_1 < 1$, the bending moment at the impact point will reach the fully plastic bending moment for initial deformation mechanism $H_1 - A_s$, and the new initial deformation mechanism $H_1 - A_{b-s}$ will appear too. The dimensionless equations of motion of segment AC are the same as Eqs. (A.11), (A.12). Eqs. (2) and (4) are still valid for segments BH_1 and H_1A.

As the yield criterion at any point in the beam should not be violated, the deformation mechanism is valid only when

$$v_{c2} < v \leq v_{c3} = \frac{95.72177}{\eta_2} \qquad 0.440237 < \eta_1 < 1$$ (A.15)

When $v_{c3} < v$ and $0.440237 < \eta_1 \leq 0.789862$, the new initial deformation mechanism is $H_1 - A_{b-s} - H_2$.

Appendix B Theoretical analysis for the dynamic behavior of a hinged-free beam struck by a rigid mass at free end

(1) $0 < v \leq v_1$ Pure shear

When value of parameter v is small, the initial deformation mechanism is shown in Fig. 12. The equations of motion of the beam are

$$\frac{d}{d\tau}\left(\frac{1}{2}\mathring{\tilde{u}}_1\right) = 2v + q_B$$ (A.16)

$$\frac{d}{d\tau}\left(\frac{1}{3}\mathring{\tilde{u}}_1\right) = 2v$$ (A.17)

where $\mathring{\tilde{u}}_1 = u_1\sqrt{mL/M_p}$. The transverse dimensionless acceleration of travelling mass is

$$\mathring{\tilde{u}}_0 = -2v/g$$ (A.18)

The dimensional bending moment distribution is found to be

$$m(x) = vx(1-x^2), \quad 0 \le x \le 1 \tag{A.19}$$

When $v = v_1 = 3\sqrt{3}/2$, the moment at $x = 3\sqrt{3}$ will reach the fully plastic bending moment and the deformation mechanism with pure shear is valid only for $0 \le v \le v_1$.

(2) $v_1 < v$ Shear-bending response

When $v_1 < v$, the deformation mechanism H_1 of the beam is shown in Fig. 13. The equation of motion can be recast as in terms of $\xi_1 = x_{h1}/l$

$$\ddot{\tilde{u}}_1 = \frac{2(4v\xi_1-3)}{\xi_1^2}, \quad \ddot{\theta}_1 = \frac{12(v\xi_1-1)}{\xi_1^3}, \quad \ddot{\phi}_1 = \frac{3}{(1-\xi_1)^3} \tag{A.20}$$

According to the acceleration condition of continuity at plastic hinge H_1, we have

$$2(3-2v\xi_1)(1-\xi_1)^2 - 3\xi_1^2 = 0 \tag{A.21}$$

The equation of motion of travelling mass is the same as Eqs. (A.18).